Available online at www.sciencedirect.com

ScienceDirect

Ceramics International 39 (2013) 8933–8940

CERAMICS INTERNATIONAL

www.elsevier.com/locate/ceramint

$MgAl_2O_4$ nanopowder synthesis by microwave assisted high energy ball-milling

H. Barzegar Bafrooei*, T. Ebadzadeh

Ceramic Division, Materials and Energy Research Center, P.O. Box 14155-4777, Tehran, Iran

Received 15 March 2013; received in revised form 22 April 2013; accepted 24 April 2013
Available online 16 May 2013

Abstract

This paper reports the development of a new process for the synthesis of spinel nano powder via microwave assisted high energy ball milling of a powder mixture containing $Al(OH)_3$ and $Mg(OH)_2$. X-ray diffraction (XRD), Simultaneous thermal analysis (STA), FTIR spectrometer, BET and scanning electron microscopy (SEM) techniques were utilized to characterize the as-milled and annealed samples. X-ray diffraction results provide evidence for the formation of a completely amorphous phase after milling for 8 h. It is found that highly ordered $MgAl_2O_4$ spinel can be obtained by calcination the as-milled powder over 800 °C. Also, SEM observations of synthesized powders showed that the particle size of powders lies in the nano meter range compared with the BET results (about 28–149 nm). The DTA–TG analyses were carried out to investigate the effect of microwave heating on the synthesis temperature compared to the conventional heat treatment by conventional furnace. Synthesis of powders with different heating methods showed that microwave heating reduces the synthesis temperature by about 200 °C.

Keywords: D. Spinel; Microwave heating; High energy ball milling; Synthesis

1. Introduction

Nanocrystalline materials with an average crystalline size of a few nanometers have been of much interest to many investigators [1–3]. Nanomaterials exhibit increased strength/hardness, enhanced diffusivity, improved ductility/toughness, reduced density and elastic modulus, increased specific heat, etc. They have high potentials for being used in structural and device applications in which enhanced mechanical and physical properties are required [4,5]. Magnesium aluminate spinel ($MgAl_2O_4$) is one of the best known and widely used materials. Showing high strength values at both elevated and normal temperatures along with the fact that it has no phase transitions up to the melting temperature (2135 °C), has made it an excellent refractory material [6]. In addition, due to its good thermal shock resistance, high chemical inertness in both acidic and basic environments, and excellent optical and dielectric properties, spinel is widely used in the metallurgical, electrochemical and chemical industrial fields [7–9]. Spinel has also found applications in dentistry [10], catalyst supports [11], humidity sensors [12], reinforcing fibers [13], photoluminescent materials [14], nuclear technology [15] and ceramic pigments [16].

High-energy ball milling (HEM, also known as mechanochemical) has been successfully used to synthesize nanocrystalline powders [17–19]. For preparing nanocrystalline ceramics, HEM offers several advantages over the other methods. Compared with high-temperature solid-state reaction technique, HEM can lower the calcination temperature due to the atomic or molecular scale homogeneity of the synthesized nanocrystalline powders [20–22]. Recently, it has been realized that microwave energy can be used to synthesize ceramic powders where reactions of component oxides at elevated temperatures are involved [23]. Microwave synthesis of materials is fundamentally different from the conventional synthesis in terms of its heating mechanism. In the microwave furnaces, heat is generated within the sample volume itself by the interaction of microwaves with the material [24]. Microwave energy heats the material on a molecular level which

*Corresponding author. Tel.: +98 263 6204130; fax: +98 263 6280030.
E-mail address: hadi.merc@gmail.com (H.B. Bafrooei).

0272-8842/$ - see front matter © 2013 Elsevier Ltd and Techna Group S.r.l. All rights reserved.
http://dx.doi.org/10.1016/j.ceramint.2013.04.089

leads to uniform heating, whereas conventional heating systems heat the material from outer surface to interior, which results in steep thermal gradients [25]. The microwave assisted preparation of nanopowders is a new method that includes hydrothermal, hydrolysis and co-precipitation methods [26–28]. In this paper, a novel approach combining ball milling and microwave heating was developed.

2. Experimental

2.1. Materials

Aluminum hydroxide ($Al(OH)_3$) and Magnesium Hydroxide ($Mg(OH)_2$) were used as the starting materials for the synthesis of $MgAl_2O_4$ spinel. All chemical materials were supplied from Merck Co. Germany. Figs. 1(a, b) and 2(a, b) shows the XRD and morphology of the initial powder agglomerates. The XRD pattern of raw materials was characterized according to those of $Al(OH)_3$ (XRD JCPDS data reference code 01-070-2038) and $Mg(OH)_2$ (XRD JCPDS data reference code 007-0239). The $Al(OH)_3$ powder has an angular shape with a mean agglomerate diameter of about 50 μm. $Mg(OH)_2$ powder has a spherical shape with a mean agglomerate size of about 5 μm. The agglomerate size of powders was determined using scanning electron microscope (SEM). Several micrographs were used for agglomerate size measurement and the average value was reported.

2.2. Experimental procedure

The milling experiment was carried out with Planetary Mill. A zirconia vial with diameter of 80 mm and 25 zirconia balls with diameter of 15 mm were used as the milling medium. The required amount of powder mixture for 15:1 ball to powder mass ratio (BPMR) was taken from the homogeneous mixture and placed in the bowl for ball milling. The raw materials were milled in air at room temperature for 0.25, 2, 4, 6 and 8 h, respectively. The rotation speed of the disk was 270 rpm and that of the vials was 675 rpm. The milled powders were calcined at 600–1100 °C by microwave heating in air.

2.3. Characterization

The structural properties of the samples were investigated by X-ray diffraction (Simens D-500 system) using a CuKα monochromatized radiation source and Ni filter in the range

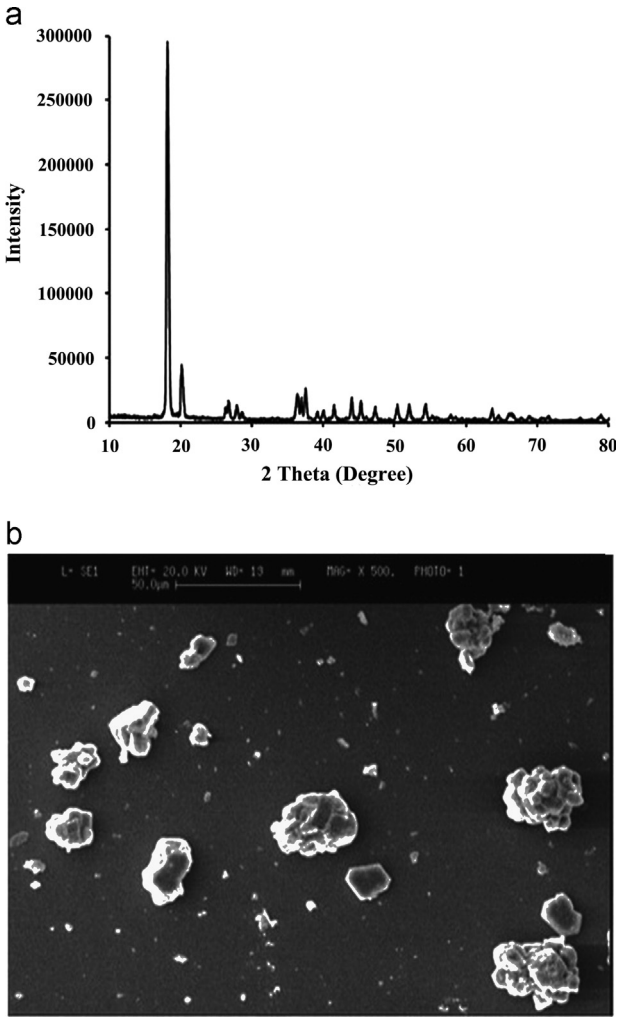

Fig. 1. (a) XRD and (b) SEM $Al(OH)_3$ powder before high energy ball milling.

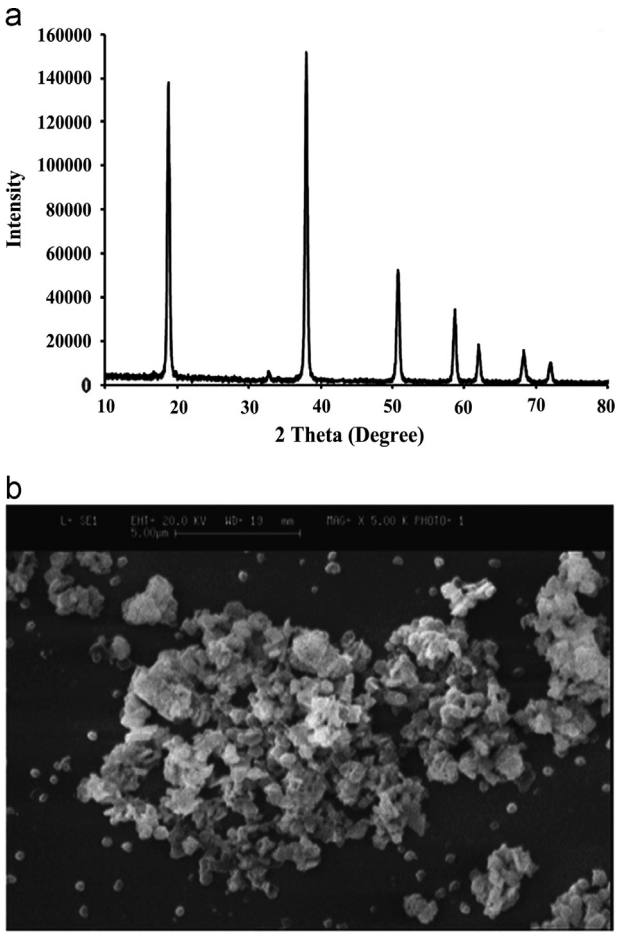

Fig. 2. (a) XRD and (b) SEM $Mg(OH)_2$ powder before high energy ball milling.

$2\theta = 10$–80. The average crystallite size (d) of the powder was estimated from the Scherrer equation (Eq. (1)):

$$d = 0.9\lambda/\beta_{sample}\cos(\theta) \quad (1)$$

where λ is the wavelength, θ is the diffraction angle, and β is the full-width for the half-maximum (FWHM) intensity peak of the powder. Three diffraction lines (311), (400) and (440) were chosen for the measurement. Thermogravimetric (TG) and differential thermal analyses (DTA) were carried out on a Netzsch STA 409 PC/PG system in flowing air atmosphere at a heating rate of 10 °C per minute. The morphology and the particle size of the high energy ball milled powders were examined by a Philips scanning electron microscope (SEM) operating at 20 kV. FTIR spectroscopy of the test materials was carried out by a Fourier transform infrared spectrometer (Bruker, V33 spectrophotometer) from 400 to 4000 cm^{-1}, using KBr pellets containing 1% weight sample in KBr. The surface areas (BET) were determined by nitrogen adsorptionat −196 °C using an automated gas adsorption analyzer (Micrometrics, Gemini 2375). The BET surface area was used to calculate the mean particle size [D] (Eq. (2)).

$$D = 6/s\rho \quad (2)$$

where 's' is the BET surface area (m^2/g) and 'ρ' is the density of spinel (kg/m^3). The density of spinel was considered as 3.59×10^3 (kg/m^3).

3. Results and discussion

Fig. 3 shows the XRD patterns for the mixtures after various milling times at room temperature. The peaks corresponding to the mixtures and the diffraction lines gradually disappeared with increased milling time and the amorphous phase was observed, as shown in Fig. 3. After a milling time of 8 h, the XRD pattern did not reveal any well-defined peaks, which indicated that the mixture was an amorphous and/or a nanocrystalline phase. The decrease of peak intensity is associated with the increase of surface defects and amorphization process during ball milling. The formation of amorphous phase through high energy ball milling was already reported in other systems [29,30]. Subsequent thermal treatments are necessary to synthesize the spinel structure. Fig. 4 shows the diffraction patterns of the powders milled during 8 h after several thermal treatments at temperatures between 600 and 1100 °C. At the lowest tested temperature (600 °C), a spinel-structured material was crystallized. As the calcination temperature increased up to 800 °C, a pure phase

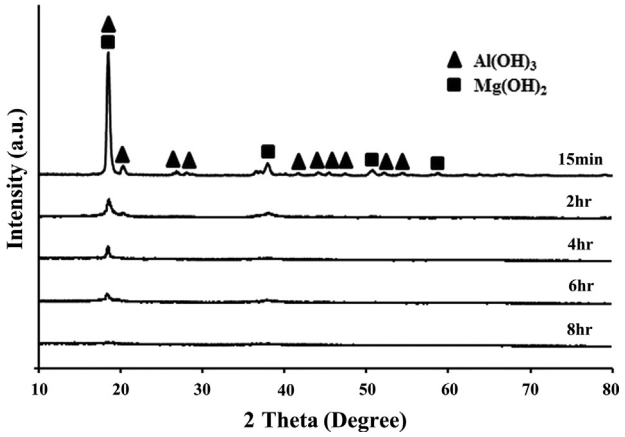

Fig. 3. The XRD patterns of the mixture of initial precursor at various ball-milling times.

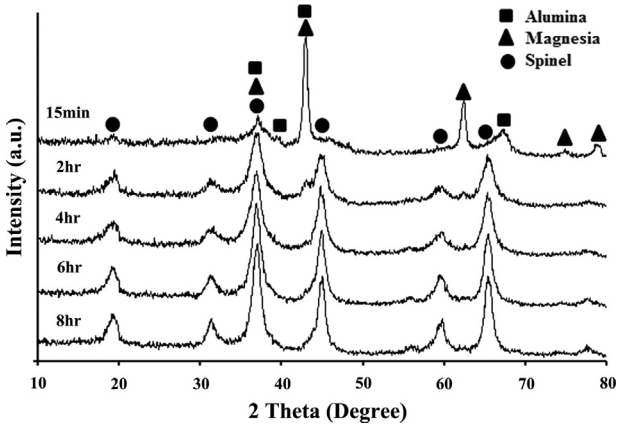

Fig. 5. XRD patterns of the mixture of initial precursors milled for different times and calcined at 800 °C by microwave processing.

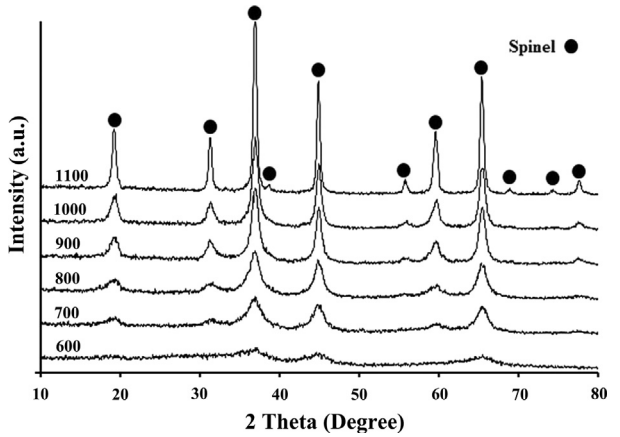

Fig. 4. XRD patterns of the mixtures initial precursors milled for 8 h and calcined at different temperatures by microwave heating.

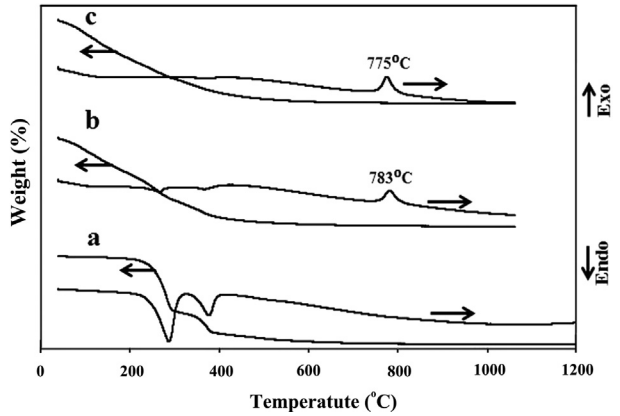

Fig. 6. STA curves of the mixtures initial precursors milled for different times: (a) 0.25 h, (b) 4 h and (c) 8 h.

spinel was obtained. However, the calcination at high temperatures resulted in the increase of peak intensity that is ascribed to the increase of crystallite size. Hence, XRD provides valuable information that the pure $MgAl_2O_4$ spinel phase can be obtained by high-energy ball milling of powders calcined at 800 °C using microwave processing. In this case, the calcination temperature decreases to 400 °C as compared to conventional solid state reaction of a high-energy ball milled powder [3]. Therefore, the calcination temperature of spinel $MgAl_2O_4$ was determined as 800 °C. Fig. 5 shows XRD patterns of the powders milled at different times and calcined at 800 °C. As observed, Al_2O_3 and MgO are dominant phases and $MgAl_2O_4$ is the minor one in

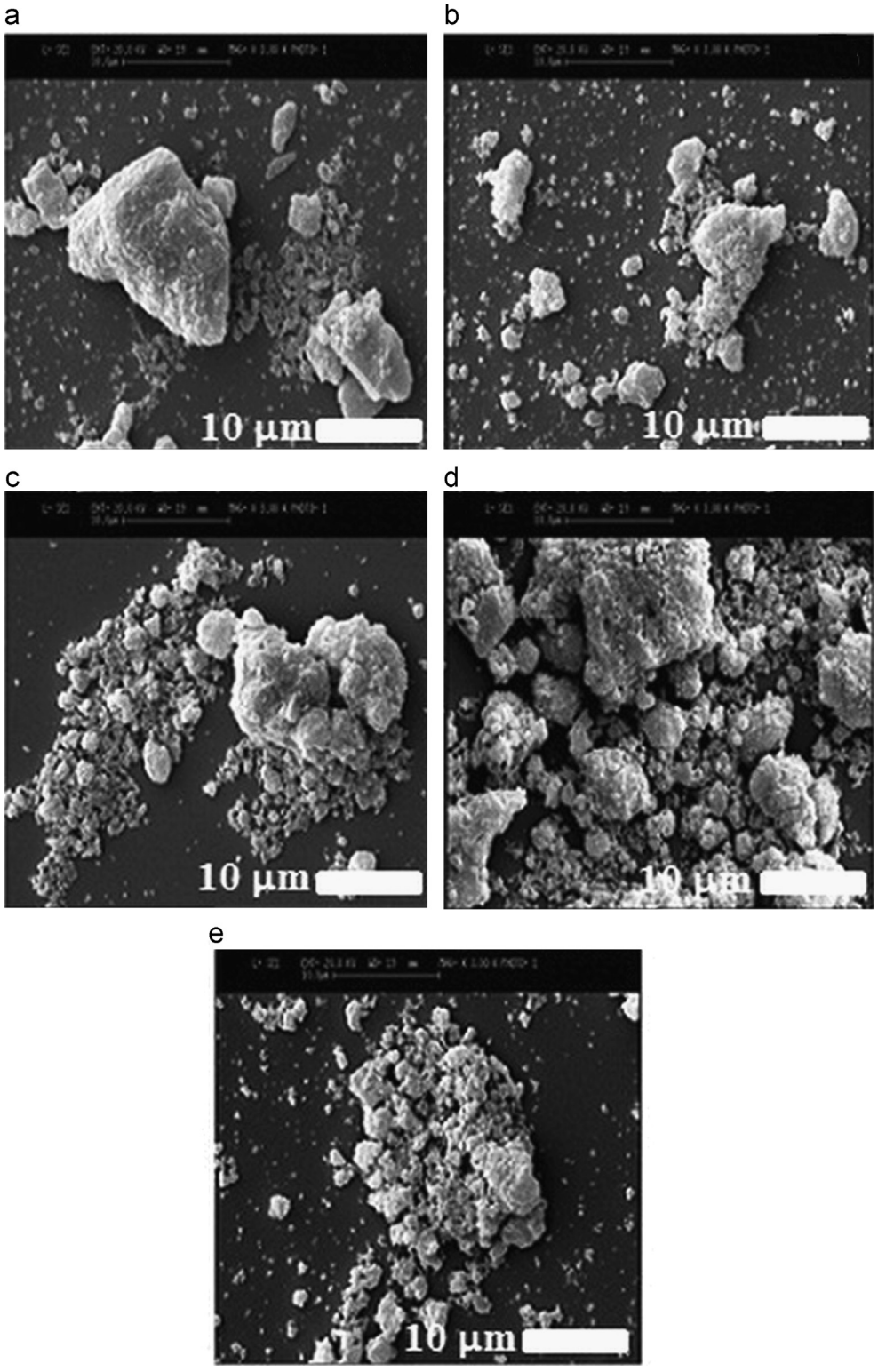

Fig. 7. SEM microghraphe of the mixture of the initial precursors milled for different times: (a) 0.25 h, (b) 2 h, (c) 4 h, (d) 6 h and (e) 8 h.

calcined powders milled for 15 min. $MgAl_2O_4$ became the only crystalline phase with a well-developed XRD pattern with increasing the milling time up to 8 h. From the above results it can be concluded that microwave assisted high energy ball milling is an effective approach to reduce the phase formation temperature of $MgAl_2O_4$, meanwhile, increasing the milling time is beneficial for obtaining the pure $MgAl_2O_4$ phase. To investigate the effect of microwave heating on formation of

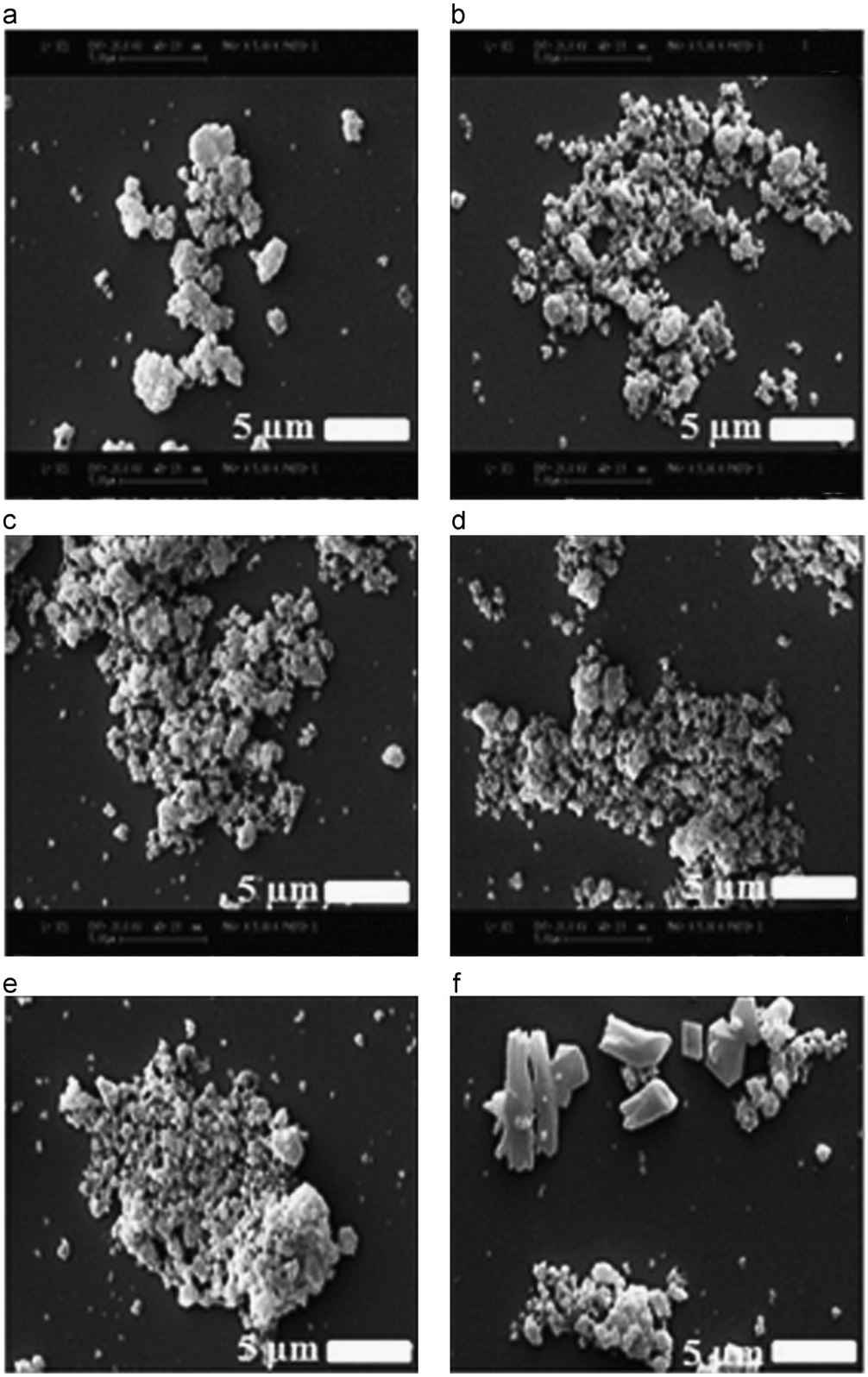

Fig. 8. SEM microghraphe of the mixtures initial precursors milled for 8 h and calcined at: (a) 600 °C, (b) 700 °C, (c) 800 °C, (d) 900 °C, (e) 1000 °C and (f) 1100 °C.

$MgAl_2O_4$ phase and compare it to the conventional heat treatment, the TG/DTA analysis was carried out and the obtained results are shown in Fig. 6. For this purpose, the mixture of initial precursors was milled for 0.25, 4 and 8 h and then subjected to DTA–TG analysis at a heating rate of 10 °C min^{-1} in air. Two endothermic peaks were clearly observed in the DTA curve of 0.25 h milled powder and they were related to $Al(OH)_3$ and $Mg(OH)_2$ decomposition. With increasing the milling time up to 4 h, the intensity of these endothermic peaks was decreased and by further increasing the milling time to 8 h, endothermic peaks disappeared completely. This can be attributed to decomposition of hydroxides during milling. The observed exothermic peak at 775 and 783 °C in powders milled for 4 and 8 h, respectively, reveals that complete formation of spinel phase occurs quite early in high-energy ball milled powder compared with that milled for 0.25 h. The weight loss of the ball milled powder for 0.25 h occurred in two main stages. The first stage occurred at a temperature below 300 °C probably due to the decomposition of $Al(OH)_3$ and crystallization of Al_2O_3. The second stage of weight loss was proven to take place below 400 °C due to the decomposition of $Mg(OH)_2$ and crystallization of MgO. There was no further significant weight loss above this temperature. The thermal analysis test results showed that the weight loss of the ball milled powder for 4 and 8 h occurred in one main stage due to decomposition of hydroxides during milling. Observations via scanning electron microscopy revealed that the milling process affects the particle morphology and sizes significantly. Fig. 7 shows the SEM micrographs of the powders milled for different times. During the milling, the particles constantly are impacted and fractured leading to a considerable reduction of the particle size as a result of the energy provided during the ball milling. Initially, they formed larger aggregates, then broken up in further steps of the milling process. Consequently, uniform grain size distribution is observed with the increase of milling time. It can be seen that the milled powders after 0.25 and 2 h contain larger particles and agglomerates but with the increase of milling time up to 4 h, the particles' and agglomerates' sizes decrease. However, with further increase of the milling time, the microstructure becomes finer and more homogenous. Fig. 7(e) shows that with the increase of milling time up to 8 h, the agglomerated particles composed of nanoparticles are more pronounced. Fig. 8 presents the SEM images of the powder high energy ball milled for 8 h and heat treated at different temperatures. After heat treatment at 600 °C, no particle coarsening occurred and the shape and size remained almost the same as those of milled powder. It can be seen that the particle sizes lightly increased as a function of calcination temperature and this is in good agreement with the crystallite size and particle size estimated using the Scherrer's equation and BET method, respectively.

Fig. 9 shows the HRSEM image of the high energy ball milled Nano powders for 8 h and heat treated at 800 °C. The samples show agglomerates of the particles consisting of

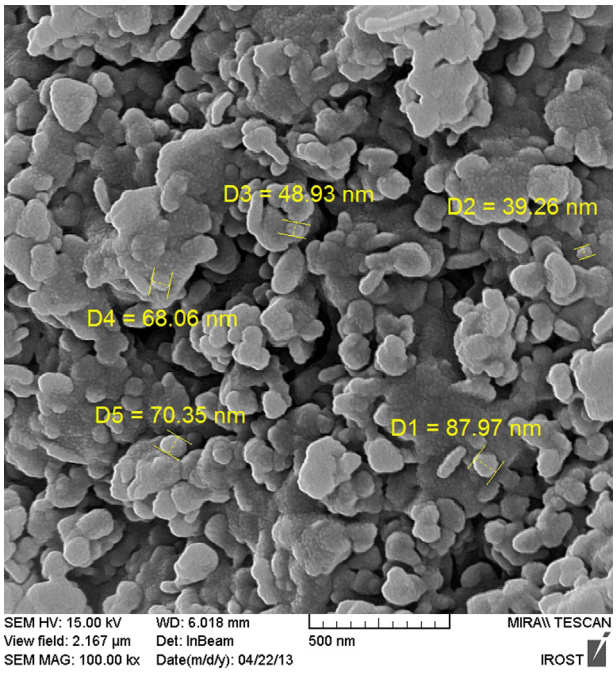

Fig. 9. HRSEM microghraphe of the mixtures initial precursors milled for 8 h and calcined at 800 °C.

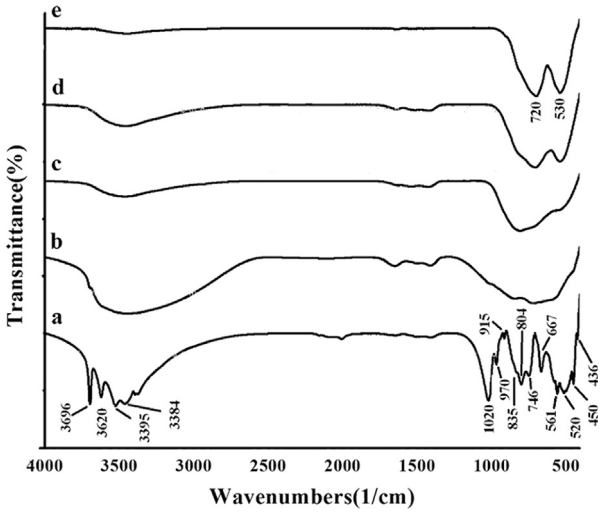

Fig. 10. FTIR spectra of ball milled mixture of initial precursors at: (a) 0.25 h, (b) 8 h and the calcined powders at (c) 600 °C, (d) 800 °C and (e) 1000 °C.

Table 1
Surface area, particle size and crystallite size of spinel nanopowders at different temperatures.

Sample	Surface area (m^2 g^{-1})	Particle size (nm)	Crystallite size (nm)
Ball milled for 8 h	14.7	–	–
Calcined at 600 °C	59.8	28	13 ± 1.5
Calcined at 700 °C	54.3	31	16 ± 1.7
Calcined at 800 °C	47.7	35	19 ± 1.6
Calcined at 900 °C	39.9	42	26 ± 1.4
Calcined at 1000 °C	24.4	68	38 ± 1.8
Calcined at 1100 °C	11.2	149	52 ± 2

slightly irregular particles with the average particle size to be less than 100 nm.

The infrared spectra of the ball milled and synthesized $MgAl_2O_4$ powders in the 4000–400 cm^{-1} range are shown in Fig. 10. For the mixture of initial precursors milled for 0.25 h, the observed bonds in the FT-IR spectrum corresponded to aluminum and magnesium hydroxides. The four high-frequency infrared bands observed in the spectra of these samples corresponded to hydroxyl group stretching vibrations of aluminum and magnesium hydroxides, which occur at 3696, 3620, 3395 and 3384 cm^{-1}. Moreover, the characteristic absorption peaks in the range of 400–1100 cm^{-1} were attributed to the bending and stretching modes of the, Al–O and Mg–O. With increasing milling time to 8 h, the intensity of bonds related to mixture of initial precursors decreased and these bonds were observed to broaden. For the calcined precursor, the IR spectrum indicates that the precursor contains an inorganic network by appearance of the two broad bands in the range of 400–800 cm^{-1}. After calcination at 600 °C, new small and two broad peaks at 720 and 530 cm^{-1} appeared due to Mg–O–Al group building up the spinel. The area and intensity of these peaks increased with raising temperature up to 1000 °C. The effect of calcination temperature on the surface area, particle size and crystallite size is shown in Table 1. The surface area increases at 600 °C (≈59.8 m^2/g); while decreases at higher temperatures. Increasing the surface area of the mixture of initial precursors is due to the rapid decomposition accompanied by the appearance of considerable stresses, which leads to decomposition of the particles. With increasing temperature from 600 to 900 °C, the surface area decreases as the particle size increases due to the grain growth. By increasing the temperature above 900 °C, the surface diffusion can be activated and caused sintering by formation of necks between particles. Therefore, the surface area reduces as the particle size increases with a higher rate above 900 °C. The mean crystallite size was determined from XRD results. As can be seen from Table 1, the crystallite size increases with increasing the temperature. In addition, the nanocrystallites grow slowly up to 900 °C and then they grow rapidly. In the case of low calcination temperature, the pores population will grow and these pores are interconnected to prevent crystallite growth [22]. Sintering mechanisms can be activated in the specimens calcined at temperatures higher than 900 °C and therefore continuous grain boundary networks have been formed due to the bridging of the fine particles. It can cause an increase in the rate of nanocrystallite growth.

4. Conclusion

In this paper, the microwave assisted high-energy ball milling technique was used to prepare nanosized magnesium-aluminate ($MgAl_2O_4$). The results showed that the single-phase $MgAl_2O_4$ was formed at the relatively low temperature of about 800 °C without unreacted Al_2O_3 and MgO phases. Powders with nanosized microstructures were formed. Also, according to TG/DTA results, the applied temperature in microwave is nearly 200 °C lower than that in conventional heat treatment. Moreover, the Scherrer's equation and BET results determined that the crystallite and particle sizes of synthesized powders lie in the range of 13–52 and 28–149 nm, respectively.

References

[1] B. Alinejad, H. Sarpoolaky, A. Beitollahi, A. Saberi, S. Afshar, Synthesis and characterization of nanocrystalline $MgAl_2O_4$ spinel via sucrose process, Materials Research Bulletin 43 (2008) 1188–1194.

[2] A. Saberi, F. Golestani-Fard, M. Willert-Porada, Z. Negahdari, C. Liebscher, B. Gossler, A novel approach to synthesis of nanosize $MgAl_2O_4$ spinel powder through sol–gel citrate technique and subsequent heat treatment, Ceramics International 35 (2009) 933–937.

[3] F. Tavangarian, R. Emadi, Mechanical activation assisted synthesis of pure nanocrystalline forsterite powder, Journal of Alloys and Compounds 485 (2009) 648–652.

[4] C. Suryanarayana, Mechanical alloying and milling, Progress in Materials Science 46 (2001) 1–184.

[5] F.H. Froes, O.N. Senkov, E. Baburaj, Synthesis of nanocristalline materials—an overview, Materials Science and Engineering A 301 (2001) 44–53.

[6] D. Mohapatra, D. Sarkar,Effect, of in situ spinel seeding on synthesis of MgO-rich $MgAl_2O_4$ composite, Journal of Materials Science 42 (2007) 7286–7293.

[7] J. Salmones, J.A. Galicia, J.A. Wang, M.A. Valenzuela, G. Aguilar-Rios, Synthesis and characterization of nanocrystallite $MgAl_2O_4$ spinels ascatalysts support, Journal of Materials Science Letters 19 (2000) 1033–1037.

[8] R. Smith, D. Bacorisen, B.P. Uberuaga, K.E. Sickafus, Dynamical simulationsof radiation damage in magnesium aluminate spinel, $MgAl_2O_4$, Journal of Physics: Condensed Matter 17 (2005) 875–891.

[9] G. Baudin, R. Martinez, P. Pena, High-temperature mechanical behaviorof stoichiometric magnesium spinel, Journal of the American Ceramic Society 78 (1995) 1857–1862.

[10] G. Cambaz, M. Timucin, Compositional modifications in humidity sensing $MgAl_2O_4$ ceramics, Key Engineering Materials 264 (2003) 1265–1268.

[11] C.W. Fairhurst, *Dental* ceramics: the state of the science, Advances in Dental Research 6 (1992) 78–81.

[12] L. Thome, A. Gentils, J. Jagielski, F. Garrido, T. Thome, Radiation stability of ceramics: test cases of zirconia and spinel, Vacuum 81 (2007) 1264–1270.

[13] S.A. Bocanegra, S.R. de Miguel, A.A. Castro, O.A. Scelza, n-Butane dehydrogenation on PtSn supported on MAl_2O_4(M: Mg or Zn) catalystsl, Catalysis Letters 96 (2004) 129–140.

[14] W. Glaubitt, W. Watzka, H. Scholz, D. Sporn, Sol–gel processing of fanctional structural ceramic oxide fibers, Journal of Sol–Gel Science and Technology 8 (1997) 29–33.

[15] V. Singh, R.P.S. Chakradhar, J.L. Rao, D.K. Kim, Synthesis characterization, photoluminescence and EPR investigations of Mn doped $MgAl_2O_4$ phosphors, Journal of Solid State Chemistry 180 (2007) 2067–2074.

[16] L.F. Koroleva, Synthesis of spinel based ceramic pigments from hydroxycarbonates, Glass and Ceramics 61 (2004) 299–302.

[17] F. Tavangarian, R. Emadi, Synthesis and characterization of pure nanocrystalline magnesium aluminate spinel powder, Journal of Alloys and Compounds 489 (2010) 600–604.

[18] A. Moure, J. Tartaj, C. Moure, Processing and characterization of Sr doped $BiFeO_3$ multiferroic materials byhigh energetic milling, Journal of Alloys and Compounds 489 (2010) 7042–7046.

[19] Z.F. Fua, P. Liua, X.M. Chena, J.L. Ma, H.W. Zhang, Low-temperature synthesis of $Mg_4Nb_2O_9$ nanopowders by high-energyball-milling method, Journal of Alloys and Compounds 493 (2010) 441–444.

[20] M.A. Sanoj, C.P. Reshmi, K.P. Sreena, Manoj Raama Varma, Sinterability and microwave dielectric properties of nano structured

$0.95MgTiO_3$–$0.05CaTiO_3$ synthesised by top down and bottom up Approaches, Journal of Alloys and Compounds 509 (2011) 3089–3095.

[21] B. Praveenkumar, G. Sreenivasalu, H.H. Kumar, D.K. Kharat, M. Balasubramanian, B.S. Murty, Size effect studies on nanocrystallinePb($Zr_{0.53}Ti_{0.47}$)O_3 synthesized bymechanical activation route, Materials Chemistry and Physics 117 (2009) 338–342.

[22] X.M. Chen, P. Liu, J.P. Zhou, W.W. Kong, J.W. Zhang, Structure and dielectric properties of Ba($Ti_{0.99}Ni_{0.01}$)O_{3-d} ceramic synthesized via high energy ball milling method, Physica B 405 (2010) 2815–2819.

[23] D. Mingos, P. Michael, Microwave syntheses of inorganic materials, Advanced Materials 5 (1993) 857–859.

[24] T. Ebadzadeh, M.H. Sarrafi, E. Salahi, Microwave-assisted synthesis and sintering of mullite, Ceramics International 35 (2009) 3175–3179.

[25] T. Ebadzadeh, Formation of mullite from precursor powders: sintering, microstructure and mechanical properties, Materials Science and Engineering A 355 (2003) 56–61.

[26] S. Barison, M. Fabrizio, S. Fasolin, F. Montagner, C. Mortalo, A microwave-assisted sol–gel Pechini method for the synthesis of $BaCe_{0.65}Zr_{0.20}Y_{0.15}O_{3-d}$ powders, Materials Research Bulletin 45 (2010) 1171–1176.

[27] H. Mohebbi, T. Ebadzadeh, F.A. Hesari, Synthesis of nano-crystalline NiO–YSZ by microwave-assisted combustion synthesis, Powder Technology 188 (2009) 183–186.

[28] N. Shojaee, T. Ebadzadeh, A. Aghaei, Effect of concentration and heating conditions on microwave-assisted hydrothermal synthesis of ZnO nanorods, Materials Characterization 61 (2010) 1418–1423.

[29] J. Xue, D. Wan, S.E. Lee, J. Wang, Mechanochemical synthesis of lead zirconatetitanate from mixed oxides, Journal of the American Ceramic Society 82 (7) (1999) 1687–1692.

[30] J.H. Shin, S.W. Choi, S.H. Hong, S.J. Kwon, S.Y. Seo, H.S. Kim, Y.H. Song, D.H. Yoon, Luminescent properties of Y(P,V)O_4:Eu^{3+} phosphors prepared by combining liquid phase precursor method and planetary ball milling, Journal of Alloys and Compounds, 509, 4331–4335.